CHEMISTRY
A EUROPEAN JOURNAL

DOI: 10.1002/chem.200601650

Donor-Functionalized Polydentate Pyrylium Salts and Phosphinines: Synthesis, Structural Characterization, and Photophysical Properties

Christian Müller,*[a] Dorothee Wasserberg,[b] Jarno J. M. Weemers,[a] Evgeny A. Pidko,[a] Sandra Hoffmann,[a] Martin Lutz,[c] Anthony L. Spek,[c] Stefan C. J. Meskers,[b] René A. J. Janssen,[b] Rutger A. van Santen,[a] and Dieter Vogt[a]

Dedicated to Professor Piet W.N.M. van Leeuwen on the occasion of his 65th birthday

Abstract: A series of donor-functionalized pyrylium salts have been prepared by classical condensation reactions which were further converted into the corresponding thienyl- and pyridyl-substituted polydentate λ^3-phosphinines by reaction with $P(SiMe_3)_3$. Further chemical modification of these phosphorus heterocycles with $Hg(OAc)_2$ in the presence of methanol resulted in the formation of λ^5-phosphinines. The photophysical properties of a selected series of thienyl- and pyridyl-functionalized pyrylium salts, λ^3- and λ^5-phosphinines, were investigated and the results compared and supported by theoretical calculations on the DFT level. Significant fluorescence was observed for the pyrylium salts and λ^5-phosphinines. In contrast, the heteroaromatic substituted λ^3-phosphinines show very little emission which is consistent with the low oscillator strength predicted by DFT calculations for this $\pi \rightarrow \pi^*$ transition. Furthermore, all three classes of compounds show readily observable phosphorescence in solution, which was determined by time-gated detection at low temperature.

Keywords: density functional calculations · fluorescence · heterocycles · phosphorescence · pyrylium salt

Introduction

λ^3- and λ^5-phosphinines (phosphorines, phosphabenzenes) are known for many decades, due to the pioneering work of Märkl, Dimroth and Ashe III in the late 1960s.[1,2] While λ^3-phosphinines are planar, aromatic heterocycles in which one -CH- group of the aryl moiety is substituted by a trivalent phosphorus atom (Figure 1, structure I), the bonding situation in λ^5-phosphinines can best be described as a superimposition of an ambivalent electronic structure: A nonclassical 6π delocalized Hückel aromatic system and a cyclic phosphonium ylide structure, having a four-coordinated phosphonium center and a negatively charged five-carbon subunit (Figure 1, structures IIa/b).[3]

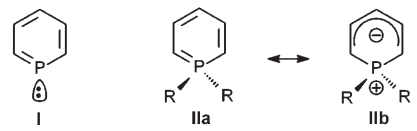

Figure 1. λ^3- and λ^5-phosphinines.

So far the organometallic chemistry of monodentate λ^3-phosphinines as ligands for transition metals has been developed considerably, but the introduction of additional donor functionalities within the phosphinine moiety has been much less regarded and reports on these systems are rare. As a matter of fact, additional donor functionalities located

[a] Dr. C. Müller, J. J. M. Weemers, E. A. Pidko, S. Hoffmann, Prof. Dr. R. A. van Santen, Prof. Dr. D. Vogt
Department of Chemical Engineering and Chemistry, Schuit Institute of Catalysis
Eindhoven University of Technology
5600 MB Eindhoven (The Netherlands)
Fax: (+31) 40-245-5054
E-mail: c.mueller@tue.nl

[b] Dr. D. Wasserberg, Dr. S. C. J. Meskers, Prof. Dr. R. A. J. Janssen
Department of Chemical Engineering and Chemistry, Molecular Materials and Nanosystems
Eindhoven University of Technology
5600 MB Eindhoven (The Netherlands)

[c] Dr. M. Lutz, Prof. Dr. A. L. Spek
Bijvoet Center for Biomolecular Research, Crystal and Structural Chemistry, Utrecht University
3584CH Utrecht (The Netherlands)

at specific positions within the phosphinine framework might provide interesting properties, such as an enhanced stability of the corresponding metal complexes due to a chelate effect, or the generation of secondary interactions through the additional donor group, with relevance for homogeneous catalytic reactions. Mathey, Le Floch and coworkers reported on thienyl-, as well as pyridyl-substituted phosphinines but their access is limited to certain substitution patterns due to the complex synthetic procedure.[4–6] During the course of our investigations on functionalized phosphinines as ligands for homogeneous catalytic reactions,[7] we started to explore the modularity of the original phosphinine synthesis via pyrylium salts, which interestingly offers an easy synthetic access to a whole variety of symmetrically as well as non-symmetrically donor-functionalized phosphinines. We report here on the preparation of thienyl- and pyridyl-functionalized pyrylium salts which were further converted into the corresponding λ^3-phosphinines by reaction with $P(SiMe_3)_3$ and fully characterized by means of NMR spectroscopy, elemental analysis and, partially, crystallographically. Because 2,4,6-aryl-substituted λ^5-phosphinines are known to show fluorescence in many cases,[2a] we further extended our investigations of phosphabenzenes with the preparation of functionalized λ^5-phosphinines substituted with additional heteroaromatic systems, which, to the best of our knowledge, have not been reported in the literature before. As a matter of fact, the incorporation of phosphorus centers in polythiophene or polypyridine chains has recently attracted a lot of interest in the field of π-conjugated materials for molecular electronics and optoelectronic applications.[8] In this context, two novel λ^5-phosphinines, substituted with additional thienyl and pyridyl groups have been prepared from the corresponding λ^3-phosphinines. The photophysical properties of these systems have been studied and compared with the corresponding λ^3-phosphinines and pyrylium salts. The results have been further compared and supported by means of DFT calculations.

Results and Discussion

Pyrylium salts and λ^3-phosphinines: Triaryl-substituted pyrylium salts can generally be synthesized either via the chalcone route (α,β-unsaturated aryl ketones, route 1 in Scheme 1) or alternatively by cyclization of 1,5-diketones in the presence of $HBF_4{\cdot}Et_2O$ or $BF_3{\cdot}Et_2O$ (route 2 in Scheme 1).[9] Nevertheless, both synthetic protocols usually have their limitations and the right reaction conditions have to be selected individually. Interestingly, both methods are not only restricted to the incorporation of phenyl substituents into the 2,6 position of the heterocycle ($R^1 = R^2 = Ph$, Scheme 1) but can also be applied for the introduction of substituted phenyl groups or even heteroaromatic substituents, such as pyridyl or thienyl groups. As a matter of fact this procedure has been investigated before to some extend for the synthesis of pyridines or pyridinium salts by reaction of substituted pyrylium salts with NH_3 or primary amines, respectively.[10] However, this modular approach has never been used for a rational design and synthesis of donor-functionalized phosphinines so far. In this respect, we further explored the incorporation of additional donor groups into the pyrylium framework and prepared the strongly fluorescent pyrylium tetrafluoroborates **4**–**7**, containing thienyl and pyridyl functionalities according to Scheme 1.[11]

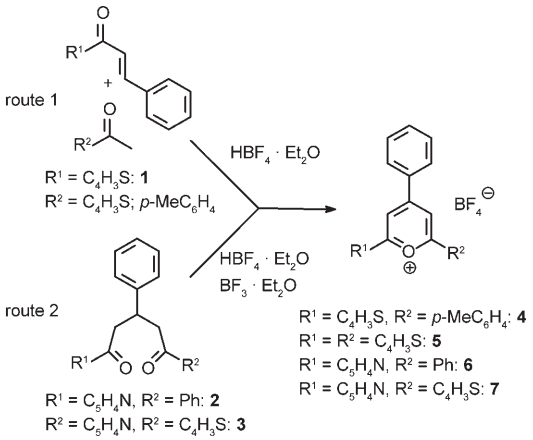

Scheme 1. Synthetic routes for the preparation of the donor-functionalized pyrylium salts **4**–**7**.

The thienyl-substituted chalcone benzal-α-acetothienone (**1**) can be prepared in high yields according to the procedure described by Weygand and Strobelt.[12] Reaction of two equivalents of **1** with *p*-methyl acetophenone in the presence of $HBF_4{\cdot}Et_2O$ in dichloroethane at 70 °C gives the thienyl substituted pyrylium salt **4** as an orange solid in 37 % yield (Scheme 1). Under similar reaction conditions the symmetrically substituted bis(thienyl)pyrylium salt **5** was obtained as a dark red solid in 21 % yield from compound **1** and 2-acetylthiophene.

Even though pyrylium salt **5** as well as the analogous ClO_4^- salt have been mentioned in the literature some decades ago, neither experimental procedures for their synthesis nor structural information has been described.[9a,11,13] Furthermore, the chalcone route (route 1, Scheme 1) provides a facile access to the BF_4^- salt and thus prevents preparation and handling of potentially explosive organic compounds.

Crystals suitable for X-ray diffraction were obtained by slow recrystallization of **5** from a fluorescent solution in methanol. Compound **5** crystallizes in the space group $P2_1/c$ with one independent molecule in the asymmetric unit. The molecular structure is depicted in Figure 2a along with selected bond lengths and angles.[14]

All aromatic rings are essentially coplanar to one another. Moreover, the bond lengths C5–C16 (1.4357(18) Å) and C1–C12 (1.4372(18) Å) are considerably shorter than a carbon–carbon single bond, indicating delocalization of the π systems over the heteroaromatic rings. In the solid state, the molecules are arranged in a herringbone-like structure as depicted in the representation of the unit-cell (Figure 2b).

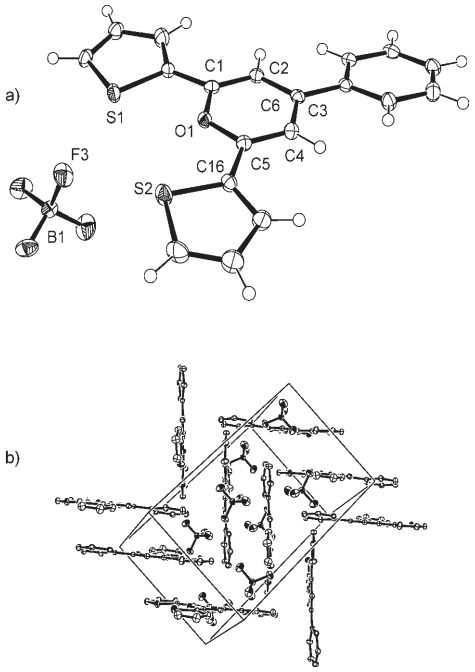

Figure 2. a) Molecular structure of **5** in the solid state (ORTEP view, 50% probability level). The thienyl ring at sulfur atom S_1 is rotationally disordered (89:11); only the major isomer is shown. Selected bond lengths [Å]: O1−C1 1.3583(15), C1−C2 1.3725(18), C2−C3 1.4100(18), C3−C4 1.4068(18), C4−C5 1.3769(18), O1−C5 1.3554(16), C3−C6 1.4799(18), C1−C12 1.4372(18), C5−C16 1.4357(18), O1−B1[i] 6.015(2) [i: 1+*x*, 0.5−*y*, 0.5−*z*]. b) Representation of the unit cell of **5** (hydrogen atoms are omitted for clarity).

The pyridyl-functionalized pyrylium salt **6** cannot be obtained directly by reaction of the chalcone benzylidene-2-acetophenone with 2-acetylpyridine and $HBF_4{\cdot}Et_2O$, due to substantial retro-aldol condensation under these reaction conditions, leading to a product mixture.[10a] However, according to a modified experimental procedure described by Katritzky et al., compound **6** was prepared starting from diketone 3,5-diphenyl-1-(2-pyridyl)pentane-1,5-dione **2** (route 2, Scheme 1).[10b,15] Subsequent oxidation with one equivalent benzylidene-2-acetophenone in the presence of $BF_3{\cdot}Et_2O$ affords the pyrylium salt **6a** as a yellow solid in 60% yield, which is most likely the bistetrafluoroborate salt containing a protonated pyridyl group.[10b] Slow recrystallization of **6a** from acetonitrile/methanol afforded bright yellow crystals. Unfortunately, no satisfying X-ray crystal structure determination of this compound could be performed, nevertheless it is certain from the X-ray data and the elemental analysis that it crystallizes as the monocationic species **6** in which the pyridyl functionality remains unprotonated.

Interestingly, we found that the diketone route (route 2, Scheme 1) is not restricted to the preparation of symmetrically substituted systems, but can also be used for the synthesis of mixed-donor functionalized pyrylium salts, with two different donor substituents attached to the heterocycle. Thus, reaction of the thienyl-functionalized chalcone benzal-α-acetothienone (**1**) with 2-acetyl-pyridine gave the corresponding diketone **3** in high yields. Subsequent oxidation with benzylidene-2-acetophenone in the presence of $BF_3{\cdot}Et_2O$ affords a dark red solid, which after recrystallization from methanol, afforded the monotetrafluoroborate pyrylium salt **7** as a yellow solid containing an unprotonated pyridyl functionality in 25% yield.[16]

The pyrylium salts **4**–**7** were further converted into the donor-functionalized phosphinines **8**–**11** by reaction with excess $P(SiMe_3)_3$ in CH_3CN.

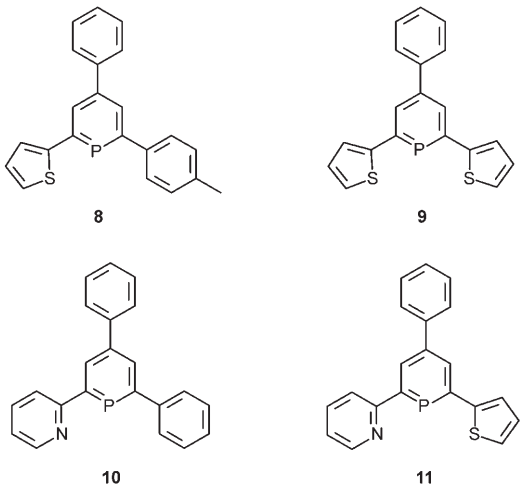

The polydentate systems were obtained as yellow, fairly air- and moisture-stable solids in moderate yields (20–46%) after column chromatography and were fully characterized by means of ^1H, ^{13}C and ^{31}P NMR spectroscopy. Analytically pure samples of all phosphinines were obtained by recrystallization from acetonitrile to afford yellow needles. In the ^{31}P NMR spectrum, all four compounds show the characteristic downfield shift of the phosphorus signal of $\delta = \approx 180$ ppm. Figure 3 shows exemplarily the ^1H and ^{31}P NMR spectra of the thienyl-functionalized phosphinine **8**.

In the ^1H NMR spectrum of **8** the two doublets at $\delta = 7.98$ and 8.16 ppm with the coupling constants of $J_{H,P} = 6.0$ and 5.6 Hz are distinctive for the P-heterocyclic protons $H_{a/b}$ of an asymmetrically substituted phosphinine and were identified by ^1H-coupled ^{31}P NMR spectroscopy. Similar observations were made for phosphinines **10** and **11**. On the other hand, the ^1H-coupled ^{31}P NMR spectrum of the symmetrically substituted bisthienyl-substituted phosphinine **9** (C_6D_6, 81 MHz) shows a single triplet at $\delta = 174.0$ ppm with a coupling constant of $J_{P,H} = 5.8$ Hz and a single doublet at $\delta = 8.03$ ppm with a coupling constant of $J_{H,P} = 5.8$ Hz (C_6D_6, 200 MHz) for the P-heterocyclic protons in the ^1H NMR spectrum. Crystals of **9** suitable for X-ray diffraction were obtained by slow recrystallization from acetonitrile. Compound **9** crystallizes in the space group *C*2/*c* with one independent molecule in the asymmetric unit and the molecular structure along with selected bond lengths and angles is depicted in Figure 4a.[17] Interestingly, the three heterocycles are essentially coplanar to one another, which was also observed in the corresponding pyrylium salt **5** (see above). In

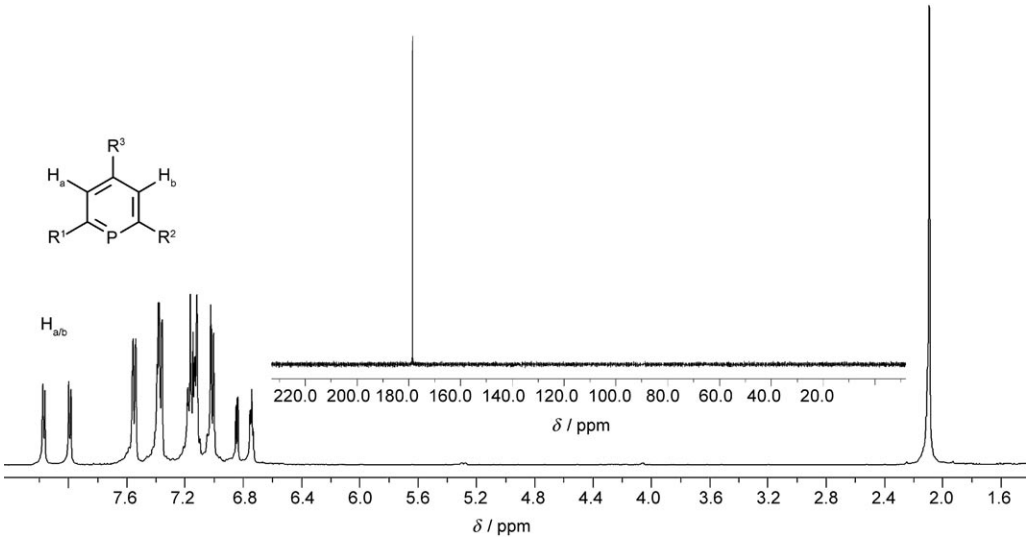

Figure 3. ^{1}H (400 MHz, C_6D_6) and ^{31}P NMR (162 MHz, C_6D_6) spectrum of the thienyl-functionalized phosphinine **8**.

contrast, the compound 2,6-bis(2-thienyl)-3-methyl-4-bromophosphinine, reported by Mathey et al., shows only one thiophene moiety strictly coplanar with the phosphorus ring, whereas the other one is twisted from the phosphinine plane. The authors describe this phenomenon as a result of steric repulsion of the five-membered sulfur heterocycle with the adjacent methyl group.[4] We further observed, that both bond lengths C1–C12 (1.470(3) Å) and C5–C16 (1.467(3) Å) in **9** are somewhat shorter than a carbon–carbon single bond, indicating at least some degree of delocalization of the aromatic systems within the three heterocycles. As observed before for the pyrylium salt **5** the molecules are packed in a herringbone structure as illustrated in Figure 4b.

In case of the pyridyl-substituted phosphinine **10** and the mixed donor-functionalized phosphinine **11** bright yellow crystals were obtained by slow recrystallization from acetonitrile. Compound **10** crystallizes in the space group $Pna2_1$ with one molecule in the asymmetric unit, which are arranged in a layer-type structure.

Unfortunately, the X-ray crystal structure analysis revealed a high degree of disorder within the molecule and therefore bond lengths and angles cannot be discussed appropriately. Nevertheless, the result is illustrated in Figure 5a, and a representation of the unit cell is depicted in Figure 5b. The crystals obtained from compound **11** were not suitable for X-ray diffraction.[18]

Alkyl-substituted bisthienyl- and pyridyl-substituted phosphinines were reported earlier by Mathey and Le Floch et al., who obtained the compounds via Pd-catalyzed Stille cross-coupling reaction of bromophosphinines with heteroaryl–trimethyltin derivatives, or by a multistep synthesis starting from five-membered phospholes. Subsequent ring-expansion with picolinoyl chloride followed by a Ni-catalyzed reduction gave the corresponding pyridyl-functionalized phosphinine as a phosphorus-containing derivative of bipyridine.[4,5] As we could demonstrate here, the described modular preparation of **8**–**11** via the pyrylium salt route provides an interesting, more convenient and less time-consuming al-

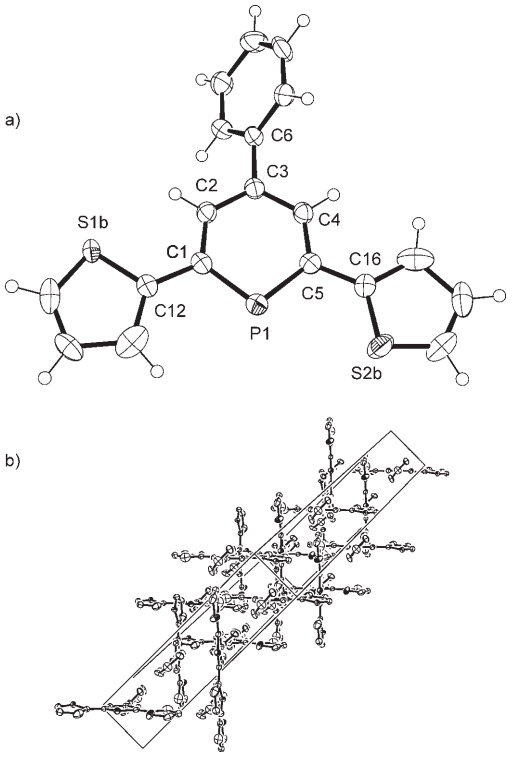

Figure 4. a) Molecular structure of **9** in the solid state (ORTEP view, 50% probability level). Both thienyl rings are rotationally disordered. Only one isomer is shown. Selected bond lengths [Å] and angles [°]: P1–C1 1.749(2), C1–C2 1.398(3), C2–C3 1.394(3), C3–C4 1.394(3), C4–C5 1.392(3), P1–C5 1.749(2), C1–C12 1.470(3), C5–C16 1.467(3), C3–C6 1.487(3), C1-P1-C5 101.37(11), C2-C3-C4: 121.5(2). b) Representation of the unit cell of **9** (hydrogen atoms are omitted for clarity, view along the crystallographic *a*,*c* diagonal).

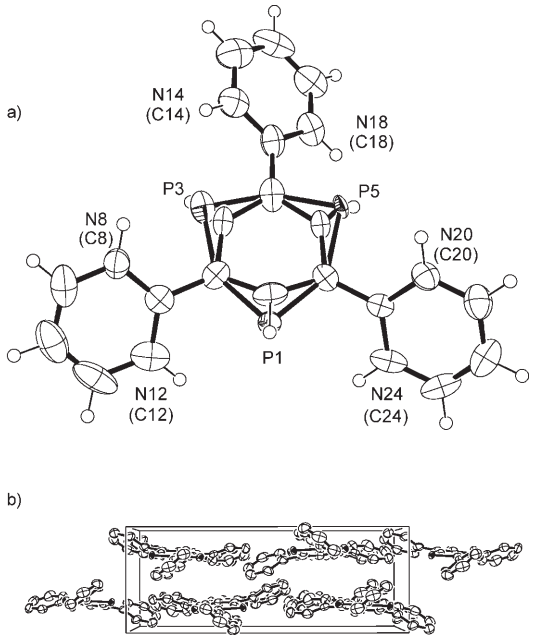

Figure 5. a) Molecular structure of **10** in the solid state (ORTEP view, 50% probability level). All N and P ring systems are disordered. b) Representation of the unit cell (hydrogen atoms are omitted for clarity, view along the crystallographic *c* axis).

ternative for the synthesis of donor-functionalized phosphinines.

λ^5 Phosphinines: The λ^3-phosphinines **9** and **11** were further converted quantitatively into the corresponding λ^5-phosphinines by reaction with $Hg(OAc)_2$ and methanol, according to the procedure described by Dimroth et al. (Scheme 2).[1d]

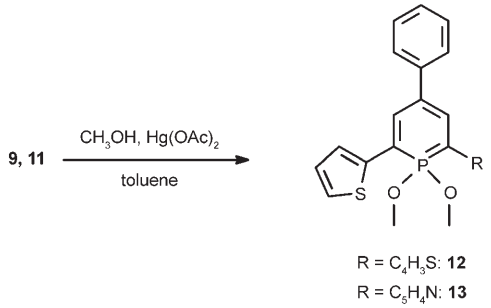

Scheme 2. Synthesis of λ^5-phosphinines **12** and **13**.

These compounds were obtained as fairly air- and moisture-stable orange and yellow solids in 80–84% isolated yield after column chromatography and were characterized by means of ^1H, ^{13}C and ^{31}P NMR spectroscopy as well as elemental analysis.[19] It should be mentioned here that thermal 1,1-elimination towards λ^3-phosphinines has been observed for certain λ^5-phosphinines and can occur especially at higher temperature, depending on the substituents.[2f,g] In the ^{31}P NMR spectrum compounds **12** and **13** show a single resonance at $\delta = 59.8$ and 62.9 ppm (C_6D_6), respectively. This high-field shift of approximately 130 ppm compared with the values of the corresponding λ^3-phosphinines is characteristic for λ^5-phosphinines.[2f,g] The ^1H NMR spectrum of **12** shows a doublet for the P-heterocyclic protons at $\delta = 8.12$ ppm with a coupling constant of $^3J_{H,P} = 36.2$ Hz, while two doublet of doublets ($\delta = 7.95$, $^3J_{H,P} = 36.0$ Hz, $^4J_{H,H} = 2.8$ Hz; $\delta = 8.34$, $^3J_{H,P} = 38.0$ Hz, $^4J_{H,H} = 2.6$ Hz) are observed for the asymmetrically substituted phosphinine **13**. The observed downfield shifts and large coupling constants compared to λ^3-phosphinines are characteristic for λ^5-phosphinines.

Photophysical properties: Because compounds **12** and **13** as well as the corresponding pyrylium salts **5** and **7** show significant yellow-green fluorescence in solution, we further recorded the electronic absorption and fluorescence spectra of the 2,6-dithienyl substituted series, **5**, **9**, **12** (SXS) and the 2-pyridyl-6-thienyl substituted series **7**, **11**, **13** (SXN) at room temperature. The low temperature absorption and phosphorescence spectra were obtained for those two series at 80 K in 2-methyltetrahydrofuran ($T = 176$ K in dichloromethane in the case of the pyrylium salts for solubility reasons). Fluorescence lifetimes and fluorescence quantum yields have further been determined at room temperature, while the phosphorescence lifetimes were estimated at low temperatures.

The electronic absorption and emission spectra reveal broad, featureless bands (Figures 6 and 7). Almost no changes were observed upon cooling the samples to low temperature, apart from a slight sharpening of the bands, which was accompanied by a slight shift of the peaks. The lowest energy (red-edge) absorption maxima (and shoulders where discernible), emission maxima as well as all mentioned photophysical data are reported in Table 1.

Within a given series (SXS, SXN) a red-shift can be observed in the electronic spectra by going from λ^3- to λ^5-phosphinines and subsequently to the pyrylium salts (Figures 6, 7, Table 1). These red-shifts within one series are more pronounced compared with compounds of the same type but of different series, that is, different substitution patterns. Generally, λ^5-phosphinines and pyrylium salts exhibit many similarities in their photophysical properties while the λ^3-phosphinines are rather different (Figures 6, 7, Table 1). The fluorescence of λ^5-phosphinines and pyrylium salts is significant (quantum yields 5–99%, Table 1) and only slightly red-shifted (by ≈ 50 nm) compared to the maximum of the lowest energy (red-edge) absorption band, from which it seems to arise. Interestingly, both λ^3-phosphinines exhibit a weak shoulder at the red-edge of the absorption spectrum. Furthermore, the two bands in the corresponding fluorescence spectra of the λ^3-phosphinines are of very low intensity (quantum yields $\ll 1\%$, Figure 7, Table 1). They seem to arise from the state that causes the shoulder at the red-edge of the absorption spectrum, as it is weak and strongly red-shifted (> 100 nm) with respect to the maximum of the lowest energy absorption band (Table 1, Figures 6, 7). How-

Table 1. Wavelengths [nm] of the transitions: $S_1 \leftarrow S_0$ at room temperature, low temperature and calculated values, $S_1 \rightarrow S_0$ at room temperature and low temperature and $T_1 \rightarrow S_0$ at low temperature and calculated values as well as fluorescence (ns) and phosphorescence [ms] lifetimes [τ] and fluorescence quantum yields [%].

Compound	Pyrylium salt		λ^3-Phosphinine		λ^5-Phosphinine	
	5	**7**	**9**	**11**	**12**	**13**
$\lambda(S_1 \leftarrow S_0)$[a] room temp. [nm]	492	457	310/391[g]	306/382[g]	446	445
$\lambda(S_1 \leftarrow S_0)$[a] low temp.[b] [nm]	499	464	312/398[g]	315/381[g]	457	455
$\lambda(S_1 \leftarrow S_0)$[a] calculations [nm]	445	421	314/376[g]	312/370[g]	394	401
$\lambda(S_1 \rightarrow S_0)$[c] room temp. [nm]	539	507	448/557[h]	448/570[h]	503	500
$\lambda(S_1 \rightarrow S_0)$[c] low temp. [nm]	535	518	450/542[h]	440/547[h]	492	496
$\lambda(T_1 \rightarrow S_0)$[d] low temp. [nm]	629	624	601	603	638	577
$\lambda(T_1 \rightarrow S_0)$[d] calculations [nm]	630	595	607	602	602	606
τ_{Fl} [ns][e]	4.84	5.27	–	–	3.59	5.36
τ_{Ph} [ms][f]	$\gg 1$	>1	≈ 1	>1	≈ 1	≈ 1
quantum yield [%]	20	99	$\ll 1$	$\ll 1$	20	5

[a] Wavelengths determined at the maximum of the lowest energy absorption band as no fine-structure was apparent. [b] 176 K for pyrylium salts (dichloromethane) and 80 K for phosphinines (2-methyltetrahydrofuran). [c] Wavelengths determined at the maximum of the emission band as no fine-structure was apparent. [d] Determined at the highest energy maximum, where discernible. [e] Measured on degassed solutions (room temperature) at 400 nm excitation wavelength, which precluded the excitation of the λ^3-phosphinines. [f] Determined using varying delay times during phosphorescence measurements. [g] First value corresponds to the maximum of the high intensity transition at the low-energy edge (red-edge) and the second value to that of the low intensity transition at the red-edge, where discernible. [h] The two values correspond to two emission bands, where discernible.

ever, due to the very low fluorescence quantum yields of the λ^3-phosphinines, especially of compound **11**, their fluorescence spectra should be interpreted with caution as effects of minor impurities could have an influence on the experimental findings, even though λ^3-phosphinines have been carefully purified by recrystallization to assure highest possible purity.

The electronic excitation energies as well as the corresponding oscillator strengths could be obtained from time-dependent density functional theory (TD-DFT) calculations. Both the theoretical and experimental absorption spectra for the SXS series are shown in Figure 6. One can see that the theoretical UV spectra reproduce the major features and general shape of the experimental spectra, while some disagreement persists for their energetic positions (Table 1).

However, one should realize that these data correspond to electronic excitations within an isolated molecule, whereas the experimental results have been obtained in the presence of a solvent. Nevertheless, the calculated absorption spectra for the λ^3-phosphinines perfectly coincide with the experimental ones in energy as much as in shape (Figure 6): the lowest energy absorption band is only weakly allowed which should give rise to a low intensity emission band (fluorescence) as indeed observed for the λ^3-phosphinines. Moreover, red-edge absorption bands of large oscillator strengths are predicted for the λ^5-phosphinines **12**

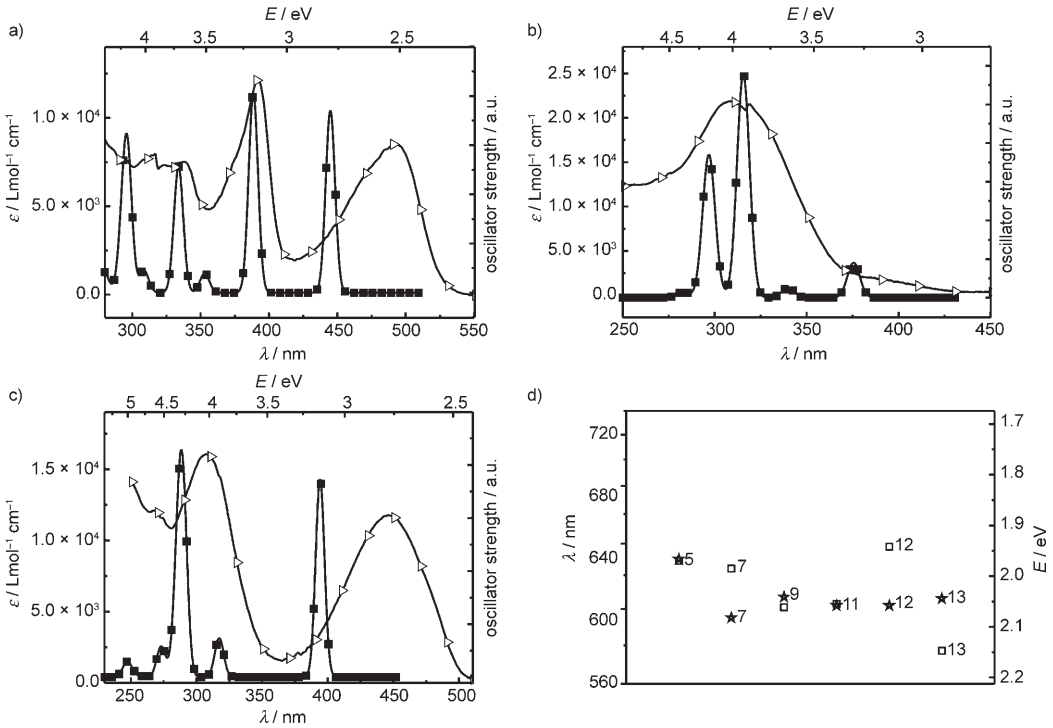

Figure 6. Comparison between experimental and theoretical results on the photophysical properties of dithienyl (SXS) and pyridylthienyl (SXN only in d). Theoretical (■, TD-DFT) versus experimental (Δ, room temperature) UV/Vis spectra of a) **5**, b) **9** and c) **12** as well as d) a comparison between theoretical (*, DFT) and experimental (□) T_1-S_0 energy gaps (designations of compounds as indicated).

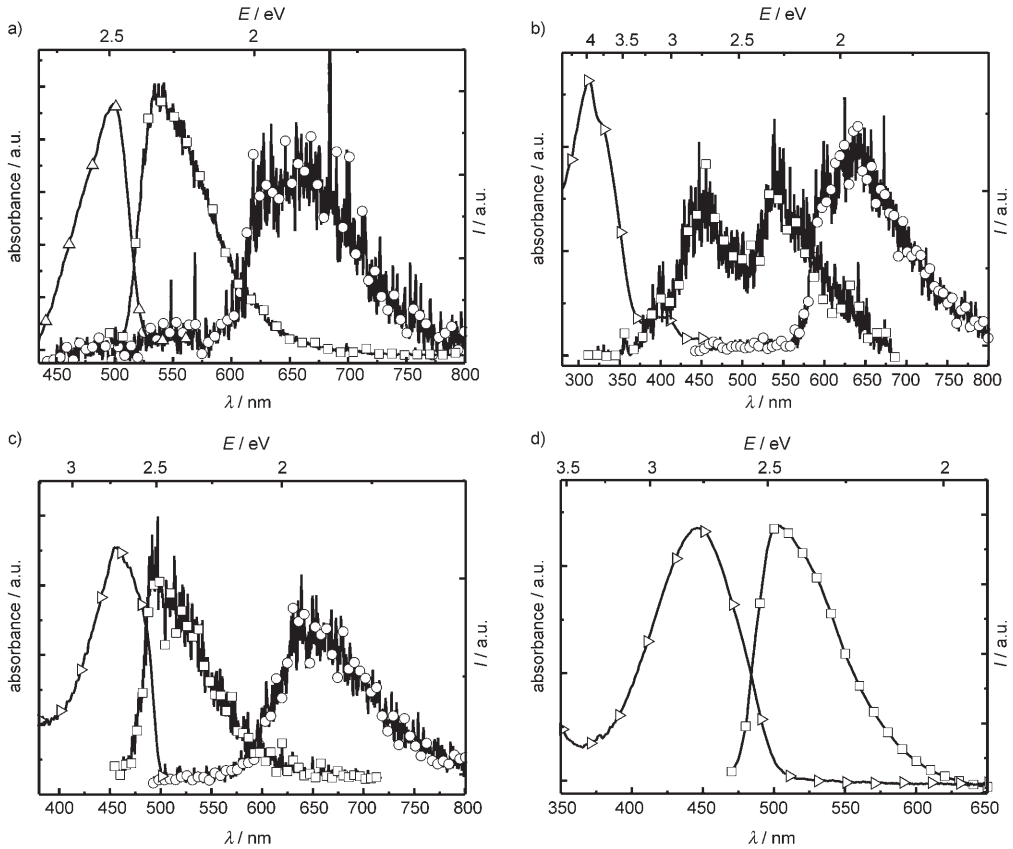

Figure 7. Low temperature UV/Vis (△), fluorescence (□) and phosphorescence (○) spectra of the SXS series: a) pyrylium salt **5** in dichloromethane 176 K; b) λ^3-phosphinine (**9**) and c) λ^5-phosphinine (**12**) in 2-methyltetrahydrofuran at 80 K; d) normalized room temperature UV/Vis (△) and fluorescence (□) spectra of λ^5-phosphinine (**12**, in 2-methyltetrahydrofuran).

and **13** and pyrylium salts **5** and **7** by theoretical calculations, which again is in agreement with the experimental findings of large intensities and high fluorescence quantum yields as well as high extinction coefficients of their lowest energy absorption bands (Figure 6).

From the theoretical calculations, we further identified the lowest energy (red-edge) absorption bands of the series SXS and SXN as $\pi \rightarrow \pi^*$ transition. In the case of the pyrylium salts and λ^5-phosphinines these transition (mainly HOMO→LUMO) are strongly allowed since they are accompanied by an apparent change of parity. Figure 8 shows the frontier orbitals involved in this process for the λ^5-phosphinine **12**.[20]

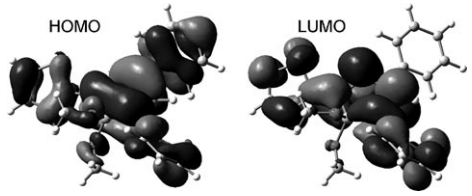

Figure 8. Representation of the frontier orbitals of the λ^5-phosphinine **12**.

On the other hand, the red-edge absorption bands for the λ^3-phosphinines **9** and **11** correspond to $\pi \rightarrow \pi^*$ transitions, rather than $n \rightarrow \pi^*$ transitions, as originally attributed to λ^3-phosphinines.[2a,21] They cause only a partial change of the orbital symmetry (Figure 9) resulting in the observed low fluorescence intensity of these compounds. As a matter of fact, for compound **9** the red-edge absorption band is a combination of the HOMO−1→LUMO and HOMO→LUMO+1 transition with the strongest contribution of the first one.

The calculations indicate that this combination results in a lower energy excitation compared with the HOMO→LUMO transitions.

The strong absorption band at 314 and 312 nm for compounds **9** and **11**, respectively, correspond to the HOMO→LUMO+1 transitions. Clearly the molecular orbitals involved (Figure 9) are very similar to those involved in the lowest energy excitations of the λ^5-phosphinines (Figure 8) leading to higher oscillator strength of the respective transitions.

Using time-gated detection, delayed luminescence spectra could readily be obtained for all compounds of the SXS (Figure 7, Table 1) and SXN (Table 1) series. These delayed

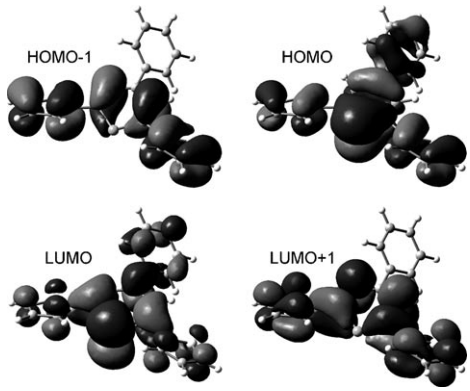

Figure 9. Representation of the frontier orbitals of the λ^3-phosphinine **9**.

luminescence spectra were interpreted as phosphorescence due to their large red-shifts > 100 nm compared with their respective absorption spectra and their very long lifetimes in the range of milliseconds (Table 1). For none of the compounds a dependence of the delayed emission on the concentration could be observed, which excludes the presence of excimers as the source of this long-lived emission. In contrast to the fluorescence measurements, phosphorescence spectra were recorded with the same ease for all six compounds, including the λ^3-phosphinines.

The energy difference between the electronic T_1 and S_0 states was also estimated based on the results of quantum-chemical calculations. Comparison of experimental and theoretical values reveals inaccuracies (those inaccuracies arising from the neglecting of vibrational effects in the calculation are deemed small compared with the accuracy of the measurement) which increase when going from λ^3- to λ^5-phosphinines and pyrylium salts (Figure 6 bottom right, Table 1). This phenomenon can be understood as the calculations assume isolated molecules in vacuum, while in the experiment the molecules are enclosed in solvent cages of finite dielectric constants. Due to the increasing ionic character in the order λ^3-, λ^5-phosphinine and pyrylium salts the error introduced by this partially charged character will be comparatively smaller for λ^3-phosphinines and comparatively larger for the λ^5-phosphinines and the salts, in agreement with the above findings. In addition to this, the low oscillator strength of the lowest of the λ^3-phosphinines' transitions precludes strong interactions with the solvent cage.

From the photophysical data presented above, it can be concluded that minor chemical changes of one heteroatom and its substitution pattern in the central ring induces distinctly different photophysical properties in the two series SXS and SXN. While considerable fluorescence (quantum yields 5–99 %) and readily detectable phosphorescence is observed for λ^5-phosphinines and pyrylium salts, the λ^3-phosphinines show very little fluorescence intensity (quantum yield $\ll 1$ %) but readily detectable phosphorescence. Furthermore, the absorption spectra corroborate the results obtained from the luminescence experiments. For λ^5-phosphinines and pyrylium salts the lowest energy absorption bands have a comparatively high extinction coefficient, while for λ^3-phosphinines the lowest energy absorption bands exhibit comparatively low extinction coefficients. These findings suggest that the energetically lowest transition is partially forbidden in the case of λ^3-phosphinines, while it is strongly allowed for λ^5-phosphinines and pyrylium salts. The theoretical UV/Vis spectra obtained from time-dependent DFT calculations support the interpretation of a partially forbidden lowest $\pi \rightarrow \pi^*$ transition of the λ^3-phosphinines as well (Figure 6, Table 1). In agreement with the experimental findings the lowest energy transitions of the λ^5-phosphinines and pyrylium salts obtained from the calculations are allowed (Figure 6, Table 1).

Conclusion

We have demonstrated, that the classical λ^3-phosphinine synthesis via pyrylium salts is not only suitable for the preparation of aryl-substituted phosphinines, but also for the incorporation of additional donor functionalities within the phosphinine framework. Due to the stepwise assembly of the phosphorus-containing heterocycle, the additional substituents can be positioned in a specific manner, allowing access to a whole variety of polydentate λ^3-phosphabenzenes with specific substitution pattern. We further showed that also donor-functionalized λ^3-phosphinines can easily be converted into the corresponding λ^5-phosphinines by simple chemical modifications. Due to the increasing interest in phosphorus-containing π-conjugated molecular materials we started to explore the photophysical properties of a selected series of thiophene- and pyridyl-substituted pyrylium salts, λ^3- and λ^5-phosphinines. The results were compared and supported by theoretical calculations on the DFT level. While the pyrylium salts as well as the λ^5-phosphinines show significant fluorescence in solution (quantum yields $\varphi = 5$–99 %, lifetimes $\tau = 3.59$–5.36 ns), the heteroaromatic substituted λ^3-posphinines show very little emission, which is attributed to a partially forbidden $\pi \rightarrow \pi^*$ transition and consistent with the low oscillator strength predicted by DFT calculations for this transition. Moreover, all three classes of compounds show readily observable phosphorescence in solution (τ in the range of milliseconds), which was determined by time-gated detection at low temperature.

We are currently investigating the influence of the additional donor functionalities on the stability of the corresponding transition metal complexes as well as the application of polydentate phosphinines in homogeneous catalysis. Due to the modularity of the λ^3- and λ^5-phosphinine synthesis we further study the possibility to tune the optoelectronic properties of the latter systems and to develop this class of compounds to novel π-conjugated organic materials.

Experimental Section

General considerations: All manipulations were carried out under an argon atmosphere, using modified Schlenk techniques unless otherwise stated. All glassware was dried prior to use by heating under vacuum. All common solvents and chemicals were commercially available and purchased from Aldrich Chemical Co. and Merck. $P(SiMe_3)_3$ was prepared according to the literature.[22] The solvents were taken from custom-made solvent purification columns filled with Al_2O_3. The elemental analyses were obtained from H. Kolbe, Mikroanalytisches Laboratorium, Mülheim a.d. Ruhr (Germany). ^1H, $^{13}C\{^1H\}$, $^{31}P\{^1H\}$ and $^{19}F\{^1H\}$ NMR spectra were recorded on a Varian Mercury 200 or 400 spectrometer and all chemical shifts are reported relative to the residual proton resonance in the deuterated solvents or referred to an 85% aqueous solution of H_3PO_4, respectively.

Photophysical experiments: 2-Methyltetrahydrofuran was pre-dried over KOH for 4 d, filtered, distilled from CaH_2, and stored under inert nitrogen atmosphere.

All sample solutions were prepared in a nitrogen glove box using dry and deoxygenated 2-methyltetrahydrofuran, toluene, ethanol or dichloromethane unless stated otherwise.

UV/Vis and photoluminescence spectra were recorded using a Perkin–Elmer Lambda 900 and an Edinburgh Instruments FS920 spectrophotometer, respectively. Time-correlated single photon counting (TC-SPC) photoluminescence was performed on an Edinburgh Instruments LifeSpec-PS spectrometer by photoexcitation at 400 nm with a picosecond-pulse laser (PicoQuant PDL 800B) operated at 2.5 MHz, 400 kHz or 40 kHz and using a Peltier-cooled Hamamatsu microchannel plate photomultiplier (R3809U-50) for detection. During the spectroscopic experiments, samples were held at room temperature or 80 K/176 K, under nitrogen atmosphere (using an Oxford Optistat CF continuous flow cryostat). The quantum yields at room temperature of λ^3-phosphinines (in 2-methyltetrahydrofuran) and pyrylium salts (in dichloromethane) were determined using *N*-(phenyl),*N*′-(1-ethylpropyl)perylenediimide (in toluene, $\varphi \approx 0.99$) as a standard. The quantum yields at room temperature of λ^3-phosphinines (in 2-methyltetrahydrofuran) were determined using 2-aminopyridine (in ethanol, $\varphi \approx 0.37$) as a standard.[23] Excitation wavelengths were identical for samples and respective standard and all respective samples had similar O.D. (< 0.1). The integrated emission spectra were corrected according to common procedure and accuracies amounted to $\pm 10\%$ due to the very low concentration required to prevent stacking.[24] Spectral resolution did not exceed 10 nm. Low temperature fluorescence and phosphorescence was recorded using gated detection. A pulsed Nd/YAG laser (Surelite II-10, Continuum, FWHM 4 ns, 10 Hz) was used for excitation combined with an optical parametric oscillator (Panther OPO, Continuum) to tune the excitation energy. Spectra were recorded with an intensified CCD camera (PI-MAX:1024HQ, Princeton Instruments) after dispersion of the emitted light by a spectrograph at gate widths of 2 ns–20 ms delay times of 2 ns–10 ns for fluorescence and >100 ns for phosphorescence to minimize residual fluorescence.

3,5-Diphenyl-1-(2-pyridyl)pentane-1,5-dione (2): The compound was prepared according to a modified literature procedure.[12] Benzylidene-2-acetophenone (8.12 g, 39.2 mmol) and 2-acetylpyridine (4.72 g, 39.2 mmol) were mixed with NaOH (1.64 g, 39.2 mmol) using a mortar and pestle. All compounds were stirred for about 10 min until a sticky yellow mixture was obtained. The product was transferred into a flask containing water/ethanol 1:2 and heated until everything was dissolved. The solution was stirred and allowed to cool down to room temperature. The pure product was filtered off and dried under vacuum, affording a white powder (11.5 g, 34.9 mmol, 89%). M.p. 104°C; for spectroscopic data see ref. [12].

1-(2-Thienyl)-3-phenyl-5-(2-pyridyl)-1,5-dione (3): Benzal-α-acetothienone (**1**) (17.7 g, 82.6 mmol) and 2-acetylpyridine (10.0 g, 82.6 mmol) were mixed with NaOH (3.3 g, 82.6 mmol) using a mortar and pestle. All compounds were stirred for about 10 min until a sticky yellow mixture was obtained. The product was transferred into a flask containing water/ethanol 1:2 and heated until everything was dissolved. The solution was stirred and allowed to cool down to room temperature. The product was filtered off and dried under vacuum, affording a yellow powder after recrystallization from ethanol/chloroform (17.5 g, 52.2 mmol, 63%). M.p. 124.8°C; ^1H NMR (200 MHz, $CDCl_3$, 25°C): $\delta = 3.32$ (m, 2H; -CH_2-), 3.73 (m, 2H; -CH_2-), 4.12 (p, $^3J_{H,H} = 7.0$ Hz, 1H; -CH-), 7.06–7.46 (m, 7H), 7.58 (d, $^3J_{H,H} = 4.0$ Hz, 1H), 7.70–7.82 (m, 2H), 7.96 (d, $^3J_{H,H} = 8.2$ Hz, 1H), 8.64 ppm (d, $^3J_{H,H} = 4.8$ Hz, 1H); ^{13}C NMR (50.3 MHz, $CDCl_3$, 25°C): $\delta = 36.9$ (-CH), 43.7, 45.9 (-CH_2-), 121.8, 126.6, 127.2, 127.6, 128.1, 128.5, 132.0, 133.6, 136.9, 143.9 (C_q), 144.4 (C_q), 148.9, 153.3 (C_q), 191.4 (C=O), 199.9 ppm (C=O); elemental analysis calcd (%) for $C_{20}H_{17}NO_2S$ (335.42): C 71.62, H 5.11, N 4.18; found: C 71.73, H 5.12, N 4.12.

2-(*p*-Methylphenyl)-6-(2-thienyl)-4-phenylpyrylium tetrafluoroborate (4): Benzal-α-acetothienone (**1**) (8.90 g, 41.35 mmol) and *p*-methylacetophenone (2.80 g, 20.76 mmol) were dissolved in CH_2Cl_2 (15 mL). The mixture was heated to 70°C and $HBF_4{\cdot}Et_2O$ (7.1 g, 41.35 mmol, 52% ethereal solution) was added dropwise. Stirring was continued at 70°C for 6 h. Subsequently, Et_2O (100 mL) was added and an orange solid precipitated, which was filtered off, washed with Et_2O and dried under vacuum (3.20 g, 7.7 mmol, 37%). M.p. 238°C; ^1H NMR (200 MHz, CD_3OD, 25°C): $\delta = 2.49$ (s, 3H, CH_3), 7.47 (t, $J_{H,H} = 5.0$ Hz, 1H), 7.53 (d, $J_{H,H} = 8.6$ Hz, 2H), 7.75 (m, 3H), 8.30 (m, 5H), 8.56 (d, $J_{H,H} = 4.0$ Hz, 1H), 8.68 ppm (d, $J_{H,H} = 5.6$ Hz, 2H); ^{13}C NMR (50.3 MHz, CD_3OD, 25°C): $\delta = 20.5$ (CH_3), 112.8, 113.0, 126.1, 128.0, 129.1, 129.8, 130.4, 130.5, 132.8, 132.9, 134.6, 135.6, 138.3, 146.9, 165.0, 166.2, 167.8, 169.2 ppm; ^{19}F NMR (188.1 MHz, $[D_4]CH_3OH$, 25°C): $\delta = -154.25$, -154.20 (3:1) ppm; elemental analysis calcd (%) for $C_{22}H_{17}BF_4OS$ (416.24): C 63.48, H 4.12; found: C 63.59, H 4.41.

2,6-(2-Thienyl)-4-phenylpyrylium tetrafluoroborate (5): Benzal-α-acetothienone (**1**) (17.44 g, 81.4 mmol) and 2-acetylthiophene (5.13 g, 40.7 mmol) were dissolved in CH_2Cl_2 (20 mL). The mixture was heated to 70°C and $HBF_4{\cdot}Et_2O$ (13.3 g, 81.4 mmol, 52% ethereal solution) was added dropwise. Stirring was continued at 70°C for 18 h. During that period a dark precipitate was formed. Et_2O (200 mL) was added and the flask was stored in the refrigerator for 36 h. The precipitate was filtered off and recrystallized from hot methanol (6.9 g, 16.9 mmol, 21%). M.p. 247.8°C; ^1H NMR (200 MHz, CD_3OD, 25°C): $\delta = 7.47$ (pseudo t, $^3J_{H,H} = 4.6$ Hz, 2H), 7.75 (m, 3H), 8.24 (d, $^3J_{H,H} = 4.8$ Hz, 2H), 8.28 (pseudo t, $^3J_{H,H} = 7.0$ Hz, 2H), 8.51 (d, $^3J_{H,H} = 4.0$ Hz, 2H), 8.62 ppm (s, 2H; heteroarom.-H); ^{13}C NMR (50.3 MHz CD_3OD, 25°C): $\delta = 112.33$, 129.06, 129.82, 130.35, 132.70 (C_q), 132.94 (C_q), 134.64 (C_q), 135.25, 138.07, 164.43 (C_q), 164.98 ppm (C_q); ^{19}F NMR (188.1 MHz, $[D_4]CH_3OH$, 25°C): $\delta = -154.70$, -154.66 (3:1) ppm; elemental analysis calcd (%) for $C_{19}H_{13}BF_4OS_2$ (408.24): C 55.90, H 3.21; found: C 56.18, H 3.19.

2-(2-Pyridyl)-4,6-diphenylpyrylium tetrafluoroborate (6): $BF_3{\cdot}Et_2O$ (22.3 g, 157.3 mmol, 8 equiv) was added dropwise to a mixture of 1,3-diphenyl-5-(2-pyridyl)-1,5-pentanedione (6.5 g, 19.7 mmol, 1 equiv) and benzylidene-2-acetophenone (4.1 g, 19.8 mmol, 1 equiv) at room temperature. The reaction mixture was then heated to 70°C for 3 h. After allowing the reaction mixture to cool down to room temperature a yellow solid precipitated after adding Et_2O. The yellow solid was collected on a glass filter, washed with Et_2O and recrystallized from methanol to obtain the pyrylium salt as yellow needles (4.7 g, 60%). M.p. 243°C (decomp); ^1H NMR (200 MHz, $[D_6]$DMSO, 25°C): $\delta = 7.90$–7.76 (m, 7H; pyridyl-H, pyryliumphenyl-$H_{m,p}$, phenyl-$H_{m,p}$), 8.26 (dt, $J_{H,H} = 7.8$ Hz, 1H; pyridyl-H), 8.79–8.49 (m, 5H; pyridyl-H, pyryliumphenyl-H_o, phenyl-H_o), 9.20 (s, 1H; pyrylium-H), 9.00 (d, $J_{H,H} = 4.4$ Hz, 1H; pyridyl-H), 9.28 ppm (s, 1H; pyrylium-H); ^{13}C NMR (50.3 MHz, $[D_6]$DMSO, 25°C): $\delta = 115.7$, 116.9, 125.0, 129.1, 129.3, 129.6, 130.4, 130.5, 132.7, 136.0, 139.1, 146.7, 151.5, 160.1, 168.2, 171.1 ppm; ^{19}F NMR (188.1 MHz, $[D_6]$DMSO, 25°C): $\delta = -148.34$ ppm; elemental analysis calcd (%) for $C_{22}H_{16}BF_4NO$ (397.18): C 66.53, H 4.06, N 3.53; found: C 67.51, H 4.13, N 3.42.

2-(2-Thienyl)-4-phenyl-6-(2-pyridyl)pyrylium tetrafluoroborate (7): A mixture of **3** (15.3 g, 45.6 mmol), benzylidene-2-acetophenone (9.5 g, 45.6 mmol), trifluoroacetic acid (6 mL) and $BF_3{\cdot}Et_2O$ (24 mL) was heated to 100°C and the dark red solution was stirred for 7 h. Subsequently, the mixture was cooled down to room temperature and Et_2O (100 mL) and acetone (100 mL) was added. Stirring was continued for

overnight. The red precipitate (**7a**, bistetrafluoroborate salt) was filtered off and dried under vacuum (6.5 g, 13.2 mmol, 29%). After recrystallization from methanol the monotetrafluoroborate salt **7** was obtained as a yellow powder (4.5 g, 11.2 mmol, 24.5%). M.p. 270.5°C; ^{1}H NMR (200 MHz, [D$_6$]DMSO, 25°C): δ=7.58 (t, $J_{H,H}$=4.2 Hz, 1H), 7.76 (m, 4H), 8.25 (t, $J_{H,H}$=7.8 Hz, 1H), 8.45 (m, 4H), 8.84 (d, $J_{H,H}$=3.6 Hz, 1H), 8.95 (d, $J_{H,H}$=4.2 Hz, 1H), 9.00 (s, 1H; heterocyclic-H), 9.13 ppm (s, 1H; heterocyclic-H); ^{19}F NMR (188.1 MHz, [D$_6$]DMSO, 25°C): δ=−148.34 ppm; elemental analysis calcd (%) for $C_{20}H_{14}BF_4NOS$ (403.20): C 59.58, H 3.50, N 3.47; found: C 59.60, H 3.60, N 3.44.

2-(*p*-Methylphenyl)-6-(2-thienyl)-4-phenyl-λ^3-phosphinine (8): $P(SiMe_3)_3$ (1.70 g, 6.8 mmol, 2.6 equiv) was added dropwise at room temperature to a stirred solution of **4** (1.1 g, 2.64 mmol, 1 equiv), dissolved in acetonitrile (10 mL). The resulting dark reaction mixture was heated to 85°C and subsequently heated under reflux for 6 h. After cooling to room temperature, the volatiles were removed under vacuum. The residue was dissolved in CH_2Cl_2 (20 mL) and added to an appropriate amount of alumina (neutral) (ca. 3–4 g). Evaporation of the solvent was followed by flash chromatography with petroleum ether/ethyl acetate 19:1 (290 mg, 0.84 mmol, 32%). M.p. 126.3°C; ^{1}H NMR (400 MHz, C_6D_6, 25°C): δ=2.09 (s, 3H, CH_3), 6.74 (m, 1H), 6.84 (d, $J_{H,H}$=5.2 Hz, 1H), 7.01 (d, $J_{H,H}$=8.0 Hz, 2H), 7.18 (m + solvent peak, 3H), 7.38 (m, 3H), 7.54 (d, $J_{H,H}$=6.8 Hz, 2H), 7.98 (d, $^3J_{H,P}$=6.0 Hz, 1H; P-heterocyclic-H), 8.16 ppm (d, $^3J_{H,P}$=5.6 Hz, 1H; P-heterocyclic-H); ^{13}C NMR (50.3 MHz, C_6D_6, 25°C): δ=20.7 (CH_3), 123.9, 124.1, 126.1, 126.2, 128.8, 129.6, 130.1 (d, $J_{C,P}$=12.0 Hz), 131.7 (d, $J_{C,P}$=12.4 Hz), 137.6 (d, $J_{C,P}$=1.9 Hz), 140.4 (d, $J_{C,P}$=25.1 Hz), 142.1 (d, $J_{C,P}$=3.1 Hz), 144.4, 144.6, 146.7 (d, $J_{C,P}$=29.8 Hz), 163.5 (d, $J_{C,P}$=51.7 Hz; C2,6), 172.1 ppm (d, $J_{C,P}$=51.7 Hz, C2/6); ^{31}P NMR (80.94 MHz, C_6D_6, 25°C): δ=178.56 ppm; elemental analysis calcd (%) for $C_{22}H_{17}PS$ (344.41): C 76.72, H 4.98; found: C 76.20, H 4.83.

2,6-(2-Thienyl)-4-phenyl-λ^3-phosphinine (9): $P(SiMe_3)_3$ (5.0 g, 20.0 mmol, 2 equiv) was added dropwise at room temperature to a stirred solution of **5** (4.0 g, 9.8 mmol, 1 equiv), dissolved in acetonitrile (20 mL) in a 100 mL Schlenk flask. The resulting dark reaction mixture was heated to 85°C and subsequently heated under reflux for 6 h. After cooling to room temperature, the volatiles were removed under vacuum. The residue was dissolved in CH_2Cl_2 (40 mL) and added to an appropriate amount of alumina (neutral) (ca. 3–4 g). Evaporation of the solvent was followed by flash chromatography with petroleum ether/ethyl acetate 9:1 (1.5 g, 4.53 mmol, 46%). M.p. 115.7°C; ^{1}H NMR (200 MHz, C_6D_6, 25°C): δ=6.71 (m, 2H), 6.81 (m, 2H), 7.13 (m + solvent peak, 3H), 7.32 (m, 4H), 8.03 ppm (d, $^3J_{H,P}$=5.8 Hz, 2H; P-heterocyclic-H); ^{13}C NMR (50.3 MHz, C_6D_6, 25°C) δ=124.03, 124.32, 126.20, 126.30, 128.85, 130.3 (d, $J_{C,P}$=12.3 Hz; C3,5), 141.7 (d, $J_{C,P}$=3.1 Hz; C4), 144.8 (d, $J_{C,P}$=13.4 Hz), 146.2 (d, $J_{C,P}$=30.3 Hz), 163.5 ppm (d, $J_{C,P}$=50.6 Hz; C2,6); ^{31}P NMR (80.94 MHz, C_6D_6, 25°C): δ=174.04 ppm; elemental analysis calcd (%) for $C_{19}H_{13}PS_2$ (336.41): C 67.84, H 3.90; found: C 67.28, H 4.13.

2-(2-Pyridyl)-4,6-diphenyl-λ^3-phosphinine (10): Under an argon atmosphere at room temperature, $P(SiMe_3)_3$ (2.8 g, 11.2 mmol, 2.1 equiv) was added dropwise to a solution of 2-(2-pyridyl)-4,6-diphenylpyrylium tetrafluoroborate (2.0 g, 5.0 mmol, 1 equiv) in acetonitrile (12 mL) in a 50 mL Schlenk flask. Upon adding a dark reaction mixture was obtained which was heated under reflux at 85°C for 6 h. Subsequently, all volatiles were removed in vacuo to obtain a dark solid. The crude product was purified by means of column chromatography over neutral alumina with ethyl acetate/petroleum ether 1:5 to afford the product as a yellow-orange solid (0.54 g, 30.7%). M.p. 146.5°C; ^{1}H NMR (200 MHz, C_6D_6, 25°C): δ=7.21–7.08 (m, 8H), 7.64 (m, 2H), 7.47 (m, 2H), 7.85 (m, 1H), 8.10 (dd, J=5.7, 1.4 Hz, 1H), 8.55 (m, 1H), 9.10 ppm (dd, J=5.7, 1.4 Hz, 1H); ^{13}C NMR (50.3 MHz, C_6D_6, 25°C): δ=120.8, 121.2, 122.4, 128.8, 132.0 (d, $J_{C,P}$=13.0 Hz; C3/5), 132.9 (d, $J_{C,P}$=11.9 Hz; C3/5), 136.2, 142.3 (d, $J_{C,P}$=3.5 Hz; C4), 143.5, 144.0, 144.2 (d, $J_{C,P}$=22.2 Hz), 149.8, 159.1 (d, $J_{C,P}$=26.1 Hz), 169.5 (d, $J_{C,P}$=50.6 Hz; C2/6), 171.5 ppm (d, $J_{C,P}$=50.6 Hz; C2/6); ^{31}P NMR (80.94 MHz, C_6D_6, 25°C): δ=187.35 ppm; elemental analysis calcd (%) for $C_{22}H_{16}NP$ (325.35): C 81.22, H 4.96, N 4.31; found: C 80.84, H 5.24, N 3.97.

2-(2-Thienyl)-4-phenyl-6-(2-pyridyl)-λ^3-phosphinine (11): $P(SiMe_3)_3$ (6.0 g, 24.0 mmol, 2 equiv) was added dropwise at room temperature to a stirred solution of **7** (4.14 g, 10.3 mmol, 1 equiv), dissolved in acetonitrile (30 mL) in a 100 mL Schlenk flask. The resulting dark reaction mixture was heated to 85°C and subsequently heated under reflux for 6 h. After cooling to room temperature, the volatiles were removed under vacuum. The residue was dissolved in CH_2Cl_2 and added to an appropriate amount of alumina (neutral) (ca. 3 g). Evaporation of the solvent was followed by flash chromatography with petroleum ether/ethyl acetate 9:1 (0.65 g, 2.0 mmol, 20%). M.p. 129.0°C; ^{1}H NMR (200 MHz, C_6D_6, 25°C): δ=6.62 (m, 1H), 6.73 (m, 1H), 6.84 (m, 1H), 7.16 (m + solvent peak, H), 7.36 (m, 1H), 7.44 (m, 2H), 7.75 (d, $^3J_{H,P}$=8.0 Hz, 1H, P-heterocyclic-H), 8.19 (dd, J=5.8, 1.2 Hz, 1H), 8.52 (d, $^3J_{H,P}$=4.9 Hz, 1H, P-heterocyclic-H), 8.94 ppm (dd, J=5.8, 1.2 Hz, 1H); ^{13}C NMR (50.3 MHz, C_6D_6, 25°C): δ=120.7, 121.0, 122.5, 123.9, 124.2, 126.0, 126.2, 127.9, 131.3 (d, $J_{C,P}$=18.5 Hz; C3/5), 132.1 (d, $J_{C,P}$=21.6 Hz; C3/5), 136.2, 142.0 (d, $J_{C,P}$=5.6 Hz; C4), 144.6 (d, $J_{C,P}$=22.2 Hz; C3), 146.8 (d, $J_{C,P}$=49.4 Hz; C2), 149.7, 158.8 (d, $J_{C,P}$=42.6 Hz; C2), 162.6, 163.6, 169.0, 170.0 ppm; ^{31}P NMR (80.94 MHz, C_6D_6, 25°C): δ=182.85 ppm; elemental analysis calcd (%) for $C_{20}H_{14}NPS$ (331.37): C 72.49, H 4.26, N 4.23; found: C 72.11, H 4.32, N 4.06.

1,1-Dimethoxy-2,6-(2-thienyl)-4-phenyl-λ^5-phosphinine (12): $Hg(OAc)_2$ (100 mg, 0.31 mmol) was suspended in dry and degassed methanol (10 mL) and cooled to −60°C. A solution of recrystallized **9** (100 mg, 0.3 mmol) in toluene (10 mL) was added and stirring was continued at room temperature for overnight. The solvents were removed in vacuo and the residue was chromatographed on neutral Al_2O_3 with toluene. The product was obtained as an orange solid (94 mg, 0.24 mmol, 80%). M.p. 135.4°C; ^{1}H NMR (200 MHz, C_6D_6, 25°C): δ=3.05 (d, $^3J_{H,P}$=13.8 Hz, 6H, O-CH_3), 6.76 (d, $J_{H,H}$=2.4 Hz, 3H), 7.14 (m, 6H), 7.51 (m, 2H), 8.12 ppm (d, $^3J_{H,P}$=36.2 Hz, 2H, P-heterocyclic-H); ^{13}C NMR (50.3 MHz, C_6D_6, 25°C): δ=52.1 (OCH_3), 87.6, 90.3, 115.8, 116.1, 122.2, 122.3, 125.0, 125.7, 138.1 (d, $J_{C,P}$=9.6 Hz), 141.5 (d, $J_{C,P}$=7.7 Hz), 142.6 ppm; ^{31}P NMR (80.94 MHz, C_6D_6, 25°C): δ=59.8 ppm; elemental analysis calcd (%) for $C_{21}H_{19}O_2PS_2$ (398.47): C 63.30, H 4.81, found: C 64.83, H 5.02 (traces of toluene).

1,1-Dimethoxy-2-(2-thienyl)-4-phenyl-6-(2-pyridyl)-λ^5-phosphinine (13): $Hg(OAc)_2$ (194 mg, 0.6 mmol) was suspended in dry and degassed methanol (12 mL) and cooled to −60°C. A solution of recrystallized **11** (198 mg, 0.5 mmol) in toluene (12 mL) was added and stirring was continued at room temperature for overnight. The solvents were removed in vacuo and the residue was chromatographed on neutral Al_2O_3 with toluene. The product was obtained as a yellow solid (165 mg, 0.42 mmol, 84%). M.p.: 107.5°C; ^{1}H NMR (200 MHz, C_6D_6, 25°C): δ=3.59 (d, $^3J_{H,P}$=13.8 Hz; O-CH_3), 7.01 (m, 2H), 7.20 (m, 3H), 7.38 (m, 2H), 7.52 (m, 2H), 7.61 (m, 2H), 7.95 (dd, $^3J_{H,P}$=36.0 Hz, $^4J_{H,H}$=2.8 Hz, 1H, P-heterocyclic-H), 8.34 (dd, $^3J_{H,P}$=38.0 Hz, $^4J_{H,H}$=2.6 Hz, 1H; P-heterocyclic-H), 8.56 ppm (m, 1H); ^{31}P NMR (80.94 MHz, C_6D_6, 25°C): δ=62.9 ppm; elemental analysis calcd (%) for $C_{22}H_{20}NO_2PS$ (393.44): C 67.16, H 5.12, N 3.56; found: C 68.50, H 5.32, N 3.36 (traces of toluene).

Crystal structure determination of 5, 9, 10: Crystals of **5**, **9** and **10** suitable for X-ray diffraction were obtained by slow recrystallization from hot methanol (**5**) or acetonitrile (**9**, **10**). Reflections were measured on a Nonius KappaCCD diffractometer with rotating anode and graphite monochromator (λ=0.71073 Å). The reflections were corrected for absorption and scaled on the basis of multiple measured reflections with the program SADABS.[25] The structures were solved with SHELXS-97 using Direct Methods[26] and refined with SHELXL-97[27] on F^2 of all reflections. Non-hydrogen atoms were refined freely with anisotropic displacement parameters. All hydrogen atoms were introduced in geometrically optimized positions and refined with a riding model. Geometry calculations, drawings and checking for higher symmetry were performed with the PLATON package.[28]

CCDC-627278 (**5**), -627279 (**9**) and -627280 (**10**) contain the supplementary crystallographic data for this paper. These data can be obtained free of charge from The Cambridge Crystallographic Data Centre via www.ccdc.cam.ac.uk/data_request/cif.

Compound 5: $[C_{19}H_{13}OS_2](BF_4)$, $F_w = 408.22$, orange-red block, $0.36 \times 0.36 \times 0.15\ mm^3$, monoclinic, $P2_1/c$ (no. 14), $a = 10.1791(4)$, $b = 10.1891(12)$, $c = 17.0876(6)$ Å, $\beta = 98.887(2)°$, $V = 1751.0(2)$ Å^3, $Z = 4$, $\rho_{calcd} = 1.549\ g\,cm^{-3}$, $\mu = 0.35\ mm^{-1}$. 50403 Reflections were measured up to a resolution of $(\sin\theta/\lambda)_{max} = 0.65$ Å^{-1} at a temperature of 110 K. 0.78–0.95 absorption correction range. 4025 Reflections were unique ($R_{int} = 0.0227$). One thienyl moiety was rotationally disordered and refined with an occupancy of 0.893:0.107. 258 Parameters were refined with eight restraints. R_1/wR_2 [$I > 2\sigma(I)$]: 0.0308/0.0801. R_1/wR_2 [all refl.]: 0.0357/0.0833. $S = 1.037$. Residual electron density between −0.31 and 0.38 e Å^{-3}.

Compound 9: $C_{19}H_{13}PS_2$, $F_w = 336.38$, yellow needle, $0.36 \times 0.06 \times 0.06\ mm^3$, monoclinic, $C2/c$ (no. 15), $a = 35.3863(5)$, $b = 5.0875(1)$, $c = 19.1892(3)$ Å, $\beta = 111.2405(6)°$, $V = 3219.91(9)$ Å^3, $Z = 8$, $\rho_{calcd} = 1.388\ g\,cm^{-3}$, $\mu = 0.42\ mm^{-1}$. 24040 Reflections were measured up to a resolution of $(\sin\theta/\lambda)_{max} = 0.62$ Å^{-1} at a temperature of 150 K. 0.92–0.98 absorption correction range. 3265 Reflections were unique ($R_{int} = 0.0557$). The thienyl and phenyl moieties were rotationally disordered and refined with occupancies of 0.64:0.36, 0.57:0.43 and 0.50:0.50, respectively. 271 Parameters were refined with 78 restraints. R_1/wR_2 [$I > 2\sigma(I)$]: 0.0425/0.1066. R_1/wR_2 [all refl.]: 0.0598/0.1175. $S = 1.069$. Residual electron density between −0.41 and 0.66 e Å^{-3}.

Compound 10: $C_{22}H_{16}NP$, $F_w = 325.33$, orange-red block, $0.36 \times 0.24 \times 0.15\ mm^3$, orthorhombic, $Pna2_1$ (no. 33), $a = 7.4375(2)$, $b = 19.8459(6)$, $c = 11.3381(2)$ Å, $V = 1673.55(7)$ Å^3, $Z = 4$, $\rho_{calcd} = 1.291\ g\,cm^{-3}$, $\mu = 0.17\ mm^{-1}$. 33035 Reflections were measured up to a resolution of $(\sin\theta/\lambda)_{max} = 0.65$ Å^{-1} at a temperature of 150 K. 0.53–0.98 absorption correction range. 2013 Reflections were unique ($R_{int} = 0.0470$). The absolute structure could not be refined reliably; thus, Friedel pairs were merged prior to the refinement. All ring systems were rotationally disordered and refined with occupancies of 0.67:0.33, 0.79:0.21 and 0.92:0.08, respectively. 244 Parameters were refined with 73 restraints. R_1/wR_2 [$I > 2\sigma(I)$]: 0.0504/0.1256. R_1/wR_2 [all refl.]: 0.0551/0.1291. $S = 1.129$.

Computational details: The quantum chemical calculations were carried out within the density functional theory using the Gaussian 03[25] program at the B3LYP/6-31G(d) level. Full geometry optimization was performed for compounds **5**, **7**, **9**, **11**, **12** and **13** both in a singlet (S_0) and triplet (T_1) state. The T_1-S_0 energy gaps were calculated as $\lambda(T_1 \rightarrow S_0) = E_{T1} - E_{S0}$, where E_{T1} and E_{S0} are the total electronic energies of the corresponding compound in the triplet and singlet state, respectively. The theoretical UV/Vis spectra were calculated at the same level of theory as the geometry optimization using the time-dependent DFT method that was implemented in the Gaussian 03 program package. Compounds **5** and **9** were modeled as isolated pyrylium cations while the influence of the counterion was neglected. Such an approximation gave better agreement between the experimental and theoretical results as compared to those obtained for the contact ion pair. Doppler broadening with a band width of 8 nm on $^1/_2$ height of the band was used for the visualization of the calculated absorption spectra.

Acknowledgements

This work was supported in part (M.L., A.L.S.) by the Council for the Chemical Sciences of the Netherlands Organization for Scientific Research (CW-NWO).

[1] a) G. Märkl, *Angew. Chem.* **1966**, *78*, 907–908; *Angew. Chem. Int. Ed. Engl.* **1966**, *5*, 846; b) A. J. Ashe III, *J. Am. Chem. Soc.* **1971**, *93*, 3293–3295; c) G. Märkl, F. Lieb, A. Merz, *Angew. Chem.* **1967**, *79*, 59; *Angew. Chem. Int. Ed. Engl.* **1967**, *6*, 458; d) K. Dimroth, W. Städe, *Angew. Chem.* **1968**, *80*, 966–967; *Angew. Chem. Int. Ed. Engl.* **1968**, *7*, 981.

[2] a) K. Dimroth, *Top. Curr. Chem.* **1973**, *38*, 1–147; b) P. Jutzi, *Angew. Chem.* **1975**, *87*, 269–283; *Angew. Chem. Int. Ed. Engl.* **1975**, *14*, 232; c) G. Märkl in *Multiple Bonds and Low Coordination in Phosphorus Chemistry* (Eds.: M. Regitz, O. J. Scherer), Thieme, Stuttgart, **1990**, pp. 220–257; d) P. Le Floch, in *Phosphorus-Carbon Heterocyclic Chemistry: The Rise of a New Domain* (Ed.: F. Mathey), Pergamon, Palaiseau, **2001**, pp. 485–533; e) F. Mathey, *Angew. Chem.* **2003**, *115*, 1616–1643; *Angew. Chem. Int. Ed.* **2003**, *42*, 1578–1604; f) K. Dimroth, *Acc. Chem. Res.* **1982**, *15*, 58–64; g) R. Streubel, *Science of Synthesis* **2005**, *15*, 1157–1179; h) K. Dimroth, *Houben-Weyl, Vol. E1*, p. 815.

[3] a) W. Schäfer, A. Schweig, K. Dimroth, H. Kanter, *J. Am. Chem. Soc.* **1976**, *98*, 4410–4418; b) Z. X. Wang, P. v. R. Schleyer, *Helv. Chim. Acta* **2001**, *84*, 1578–1600.

[4] P. Le Floch, D. Carmichael, L. Ricard, F. Mathey, *J. Am. Chem. Soc.* **1993**, *115*, 10665–10670.

[5] J. M. Alcaraz, A. Brèque, F. Mathey, *Tetrahedron Lett.* **1982**, *23*, 1565–1568.

[6] For methoxy- and hydroxy-functionalized phosphinines see: B. Breit, R. Winde, T. Mackewitz, R. Paciello, K. Harms, *Chem. Eur. J.* **2001**, *7*, 3106–3121 and ref. [7].

[7] C. Müller, L. Guarrotxena López, H. Kooijman, A. L. Spek, D. Vogt, *Tetrahedron Lett.* **2006**, *47*, 2017–2020.

[8] a) T. Baumgartner, R. Réau, *Chem. Rev.* **2006**, *106*, 4681–4727; b) H.-C. Su, O. Fadhel, C.-J. Yang, T.-Y. Cho, C. Fave, M. Hissler, C.-C. Wu, R. Réau, *J. Am. Chem. Soc.* **2006**, *128*, 983–995; c) J. Casado, R. Réau, J. T. López Navarrete, *Chem. Eur. J.* **2006**, *12*, 3759–3767; d) T. Baumgartner, W. Wilk, *Org. Lett.* **2006**, *8*, 503–506; e) N. H. T. Huy, E. Perrier, L. Ricard, F. Mathey, *Organometallics* **2006**, *25*, 5176–5179; f) T. Baumgartner, W. Bergmans, T. Kárpárti, T. Neumann, M. Nieger, M. Nyulászi, *Chem. Eur. J.* **2005**, *11*, 4687–4699; g) L. Zhang, M. Hissler, H.-B. Bu, P. Bäuerle, C. Lescop, R. Réau, *Organometallics* **2005**, *24*, 5369–5376; h) C. Fave, M. Hissler, T. Kárpáti, J. Rault-Berthelot, V. Deborde, L. Toupet, L. Nyulászi, R. Réau, *J. Am. Chem. Soc.* **2004**, *126*, 6058–6063; i) T. Baumgartner, T. Neumann, B. Wirges, *Angew. Chem.* **2004**, *116*, 6323–6328; *Angew. Chem. Int. Ed.* **2004**, *43*, 6197–6201; j) C Fave, T.-Y. Cho, M. Hissler, C.-W. Chen, T.-Y. Luh, C.-C. Wu, R. Réau, *J. Am. Chem. Soc.* **2003**, *125*, 9254–9255; k) C. Hay, C. Fave, M. Hissler, J. Rault-Berthelot, R. Réau, *Org. Lett.* **2003**, *5*, 3467–3470; l) C. Hay, M. Hissler, C. Fischmeister, J. Rault-Berthelot, L. Toupet, L. Nyulászi, R. Réau, *Chem. Eur. J.* **2001**, *7*, 4222–4236; m) C. Hay, C. Fischmeister, M. Hissler, L. Toupet, R. Réau, *Angew. Chem.* **2000**, *112*, 1882–1885; *Angew. Chem. Int. Ed.* **2000**, *39*, 1812–1815.

[9] a) G. N. Dorofeenko, G. A. Korol′chenko, S. V. Krivun, *Khim. Geterotsikl. Soedin.* **1965**, *6*, 817–821; b) J. A. VanAllan, G. A. Reynolds, *J. Org. Chem.* **1968**, *33*, 1102–1105; c) S. S. Lin, C. Y. Li, X. Wang, *Chin. Chem. Lett.* **2002**, *13*, 605–606.

[10] a) A. R. Katritzky, S. S. Thind, *J. Chem. Soc. Perkin Trans. 1* **1980**, 1895–1900; b) A. R. Katritzky, E. M. Elisseou, R. C. Patel, B. Plau, *J. Chem. Soc. Perkin Trans. 1* **1982**, 125–130; c) K. Dimroth, C. Reichardt, K. Vogel, *Org. Synth. Coll. Vol. V*, 1135–1137; d) A. R. Katritzky, J. M. Lloyd, R. C. Patel, *J. Chem. Soc. Perkin Trans. 1* **1982**, 117–123.

[11] Pyrylium salts show in many cases strong fluorescence in solution and have been used as laser dyes. See for example: D. Basting, F. P. Schäfer, B. Steyer, *Appl. Phys.* **1974**, *3*, 81–88.

[12] C. Weygand, F. Strobelt, *Chem. Ber.* **1935**, *68*, 1839–1847.

[13] A. R. Katritzky, M. Rezende, *J. Chem. Res.* **1980**, 312–313.

[14] For the crystal and molecular structure of pyrylium salts see also: a) M. Gdaniec, I. Turowksa-Tyrk, T. M. Krygowski, *J. Chem. Soc. Perkin Trans. 2* **1989**, 613–616; b) I. Turowska-Tyrk, T. M. Krygowski, P. Milart, G. Butt, R. D. Topsom, *J. Mol. Structure* **1991**, *245*, 289–299; c) I. Turowska-Tyrk, T. M. Krygowski, P. Milart, *J. Mol. Structure* **1991**, *263*, 235–245; d) I. Turowska-Tyrk, R. Anulewicz, T. M. Krygowski, B. Pniewska, P. Milart, *Pol. J. Chem.* **1992**, *66*, 1831.

[15] G. W. V. Cave, C. L. Raston, *J. Chem. Soc. Perkin Trans. 1* **2001**, 3258–3264.

[16] Bright-yellow crystals of **7** were obtained by slow recrystallization from acetonitrile but no satisfactory X-ray crystal structure determi-

nation could be performed. However, the X-ray data show that **7** crystallizes as the monotetrafluoroborate pyrylium salt.

[17] For X-ray structures of λ^3-phosphinines see for example: a) W. Fischer, E. Hellner, A. Chatzidakis, K. Dimroth, *Tetrahedron Lett.* **1968**, *59*, 6227–6230; b) J. C. J. Bart, J. J. Daly, *Angew. Chem.* **1968**, *80*, 843–844; *Angew. Chem. Int. Ed. Engl.* **1968**, *7*, 811; c) G. Maas, J. Fink, H. Wingert, K. Blatter, M. Regitz, *Chem. Ber.* **1987**, *120*, 819; d) N. Avavari, N. Mézailles, L. Ricard, P. Le Floch, F. Mathey, *Science* **1998**, *280*, 1587–1589; e) S. Choua, C. Dutan, L. Cataldo, T. Berclaz, M. Geoffroy, N. Mézailles, A. Moores, L. Ricard, P. Le Floch, *Chem. Eur. J.* **2004**, *10*, 4080–4090; f) C. Müller, M. Lutz, A. L. Spek, D. Vogt, *J. Chem. Crystallogr.* **2006**, *36*, 869–874.

[18] Bright yellow crystals of **11** were further obtained by recrystallization from hot CH_3CN and were subject to an X-ray crystal structure analysis. However, due to a high degree of disorder the structure could not be refined sufficiently.

[19] For a structural characterization of a λ^5-phosphinine see: U. Thewalt, C. E. Bugg, *Acta Crystallogr.* **1972**, *B28*, 871–879.

[20] For the nature of bonding in λ^5-phosphinines see ref. [2f] and: W. Schäfer, A. Schweig, K. Dimroth, H. Kanter, *J. Am. Chem. Soc.* **1976**, *98*, 4410–4418.

[21] For the nature of bonding in λ^3-phosphinines see for example: a) H. Oehling, A. Schweig, *Tetrahedron Lett.* **1970**, *56*, 4941–4944; b) H. Oehling, W. Schäfer, A. Schweig, *Angew. Chem.* **1971**, *83*, 723–725; *Angew. Chem. Int. Ed. Engl.* **1971**, *10*, 656–657; c) A. Schweig, W. Schäfer, *Phosphorus* **1972**, *1*, 203; d) A. Schweig, W. Schäfer, K. Dimroth, *Angew. Chem.* **1972**, *84*, 1146–1147; *Angew. Chem. Int. Ed. Engl.* **1972**, *11*, 631–636; e) C. Batich, E. Heilbronner, V. Hornung, A. J. Ashe III, D. T. Clark, U. T. Cobley, D. Kilcast, I. Scanlan, *J. Am. Chem. Soc.* **1973**, *95*, 928–930; f) E. F. DiMauro, M. C. Kozlowski, *J. Chem. Soc. Perkin Trans. 1* **2002**, 439.

[22] E. Nieke, H. Westermann, *Synthesis* **1988**, 330.

[23] T. Mutai, J.-D. Cheon, G. Tsuchiya, K. Araki, *J. Chem. Soc. Perkin Trans. 2* **2002**, 862–865.

[24] D. F. Eaton, *Pure Appl. Chem.* **1988**, *60*, 1107–1114.

[25] G. M. Sheldrick, SADABS: Area-Detector Absorption Correction, v2.10, Universität Göttingen (Germany), **1999**.

[26] G. M. Sheldrick, SHELXS-97. Program for crystal structure solution, University of Göttingen (Germany), **1997**.

[27] G. M. Sheldrick, SHELXL-97. Program for crystal structure refinement, University of Göttingen (Germany), **1997**.

[28] A. L. Spek, *J. Appl. Crystallogr.* **2003**, *36*, 7–13.

[29] Gaussian 03, Revision B.05, M. J. Frisch, G. W. Trucks, H. B. Schlegel, G. E. Scuseria, M. A. Robb, J. R. Cheeseman, J. A. Montgomery, Jr., T. Vreven, K. N. Kudin, J. C. Burant, J. M. Millam, S. S. Iyengar, J. Tomasi, V. Barone, B. Mennucci, M. Cossi, G. Scalmani, N. Rega, G. A. Petersson, H. Nakatsuji, M. Hada, M. Ehara, K. Toyota, R. Fukuda, J. Hasegawa, M. Ishida, T. Nakajima, Y. Honda, O. Kitao, H. Nakai, M. Klene, X. Li, J. E. Knox, H. P. Hratchian, J. B. Cross, C. Adamo, J. Jaramillo, R. Gomperts, R. E. Stratmann, O. Yazyev, A. J. Austin, R. Cammi, C. Pomelli, J. W. Ochterski, P. Y. Ayala, K. Morokuma, G. A. Voth, P. Salvador, J. J. Dannenberg, V. G. Zakrzewski, S. Dapprich, A. D. Daniels, M. C. Strain, O. Farkas, D. K. Malick, A. D. Rabuck, K. Raghavachari, J. B. Foresman, J. V. Ortiz, Q. Cui, A. G. Baboul, S. Clifford, J. Cioslowski, B. B. Stefanov, G. Liu, A. Liashenko, P. Piskorz, I. Komaromi, R. L. Martin, D. J. Fox, T. Keith, M. A. Al-Laham, C. Y. Peng, A. Nanayakkara, M. Challacombe, P. M. W. Gill, B. Johnson, W. Chen, M. W. Wong, C. Gonzalez, J. A. Pople, Gaussian, Inc., Pittsburgh PA, **2003**.

Received: November 17, 2006
Published online: March 9, 2007

